Engineering Microbiology 3 (2023) 100057

Contents lists available at ScienceDirect

Engineering Microbiology

journal homepage: www.elsevier.com/locate/engmic

Original Research Article

Synergistic antifungal mechanism of effective components from essential oil against *Penicillium roqueforti*

Fangyuan Zhao[a,b,c], Qianyu Li[a,b,c], Hao Wu[a,b,c], Jinglin Huang[a,b,c], Jian Ju[a,b,c,*]

[a] *Special Food Research Institute, Qingdao Agricultural University, Qingdao 266109, China*
[b] *Qingdao Special Food Research Institute, Qingdao 266109, China*
[c] *Key Laboratory of Special Food Processing (Co-construction by Ministry and Province), Ministry of Agriculture Rural Affairs, China*

ARTICLE INFO

Keywords:
Essential oil
Antifungal mechanism
Molecular docking
Molecular potential

ABSTRACT

Essential oil (EO) has significant antifungal activity. However, there is limited information on the mechanism of the synergistic antifungal effect of the effective components of EO against fungi. In the present study, molecular electrostatic potential and molecular docking were used for the first time to investigate the synergistic antifungal mechanism of eugenol and citral small molecule (C_{EC}) against *Penicillium roqueforti*. The results showed that the C_{EC} treatment made the activity of β-(1,3)-glucan synthase (GS) and chitin synthase (CS) decreas by 20.2% and 11.1%, respectively, and the contents of which decreased by 85.0% and 27.9%, respectively compared with the control group. Molecular docking revealed that C_{EC} small molecules could bind to GS and CS through different amino acid residues, inhibiting their activity and synthesis. The C_{EC} can combine with tryptophan, tyrosine, and phenylalanine in the cell membrane, causing damage to the cell membrane. The binding sites between small molecules and amino acids were mainly around the OH group. In addition, C_{EC} affected the energy metabolism system and inhibited the glycolysis pathway. Simultaneously, C_{EC} treatment reduced the ergosterol content in the cell membrane by 58.2% compared with the control group. Finally, changes in β-galactosidase, metal ion leakage, and relative conductivity confirmed the destruction of the cell membrane, which resulted in the leakage of cell contents. The above results showed that C_{EC} can kill *P. roqueforti* by inhibiting energy metabolism and destroying the integrity of the cell membrane.

1. Introduction

Mold is a type of fungus with a large population, a fast metabolism, and a strong reproductive ability, that enables it to grow and reproduce easily in a humid environment and suitable temperature [5]. *Penicillium roqueforti* is a foodborne fungus that is resistant to acid, hypoxia, and high concentration of carbon dioxide. It has a high detection rate in cereals, traditional Chinese medicine, feed and cheese [18,23]d. Simultaneously, it can pollute baked goods, meat products and low-temperature preserved foods [15]. Furthermore, *P. roqueforti* can metabolize and produce toxins such as Penicillin Roquefort toxin, roquefortine C, and mycophenolic acid. The ingestion of contaminated food by humans or animals usually causes symptoms such as vomiting, diarrhea, and gastroenteritis and can even cause death in severe cases [20]. Therefore, the fungal contamination caused by *P. roqueforti* causes significant economic losses to agricultural production, and poses a serious hazard to human health.

Effective measures to control fungal contamination must be implemented to ensure the quality and safety of agricultural products. Furthermore, most countries continue to employ synthetic preservatives such as pyrrole benzenes, imidazole, and thiocyanates, which have shown promising results in controlling postharvest fungi and mycotoxins in agricultural products [15]. However, with an increasing demand for more clearly-labeled, “chemical-free” and “natural” products, some chemical preservatives are increasingly being banned [15]. Therefore, there is a dire need to develop safe and effective antifungal agents due to the seriousness of fungal contamination and the urgency of controlling fungal pollution.

Plant essential oils (EOs) have attracted the attention of researchers due to their broad-spectrum antibacterial activity [17,33]. The EO has been used in the food industry as a natural seasoning and can meet the requirements of consumers for the safety of food additives [24]. Furthermore, cinnamon EO could significantly inhibit the growth of *Penicillium roqueforti* and *Aspergillus niger* and extend the shelf life of baked goods [14]. Similarly, lemon EO could inhibit the growth of *P. roqueforti* and *A. niger* in bread during storage [6]. Citronella EO steam could promote the growth of *Penicillium corylophilum*. Simultaneously, the author demonstrated that the EO could be used to extend the shelf life of beef jerky [12]. In addition, essential oils and their active components

* Corresponding author.
E-mail address: jujian0808@163.com (J. Ju).

https://doi.org/10.1016/j.engmic.2022.100057
Received 24 June 2022; Received in revised form 27 October 2022; Accepted 31 October 2022
Available online 2 November 2022

have good antifungal activity, and biodegradability, which can compensate for a few of the disadvantages of chemically synthesized antifungal agents [13,16]. In addition, clove and Litsea cubeba essential oils have eugenol and citral as the main active components, respectively [25,27]. Several reports have demonstrated the significant antimicrobial activity of clove and Litsea cubeba essential oils [2,19,26,31]. However, these studies primarily focused on the active components of a single essential oil. There has been limited research on the synergistic antifungal activity of the effective components of essential oils. Therefore, in the present study, molecular electrostatic potential and molecular docking were combined for the first time to investigate the synergistic antifungal mechanism of the C_{EC} against *P. roqueforti*. Furthermore, this research can provide the scientific basis for further development of natural antifungal agents with synergistic antifungal activities.

2. Materials and methods

2.1. Materials and reagents

P. roqueforti (ATCC 10110) was purchased from China Microbial Strain Preservation and Management Center (Beijing, China). Eugenol (CAS-No.97-53-0, biotechnology grade, purity 98%) and citral (CAS-No.5392-40-5, biotechnology grade, purity 95%) were purchased from Ballingway Technology Co., Ltd. (Shanghai). Potato Dextrose Agar (PDA) and Potato Dextrose Broth (PDB) were purchased from Shandong Tuopu Bioengineering Co., Ltd. (Qingdao). Anhydrous ethanol (AR grade, purity ≥ 99.7%) and all other chemical reagents were procured from Sinopharm Group Chemical Reagent Co., Ltd. (Shanghai).

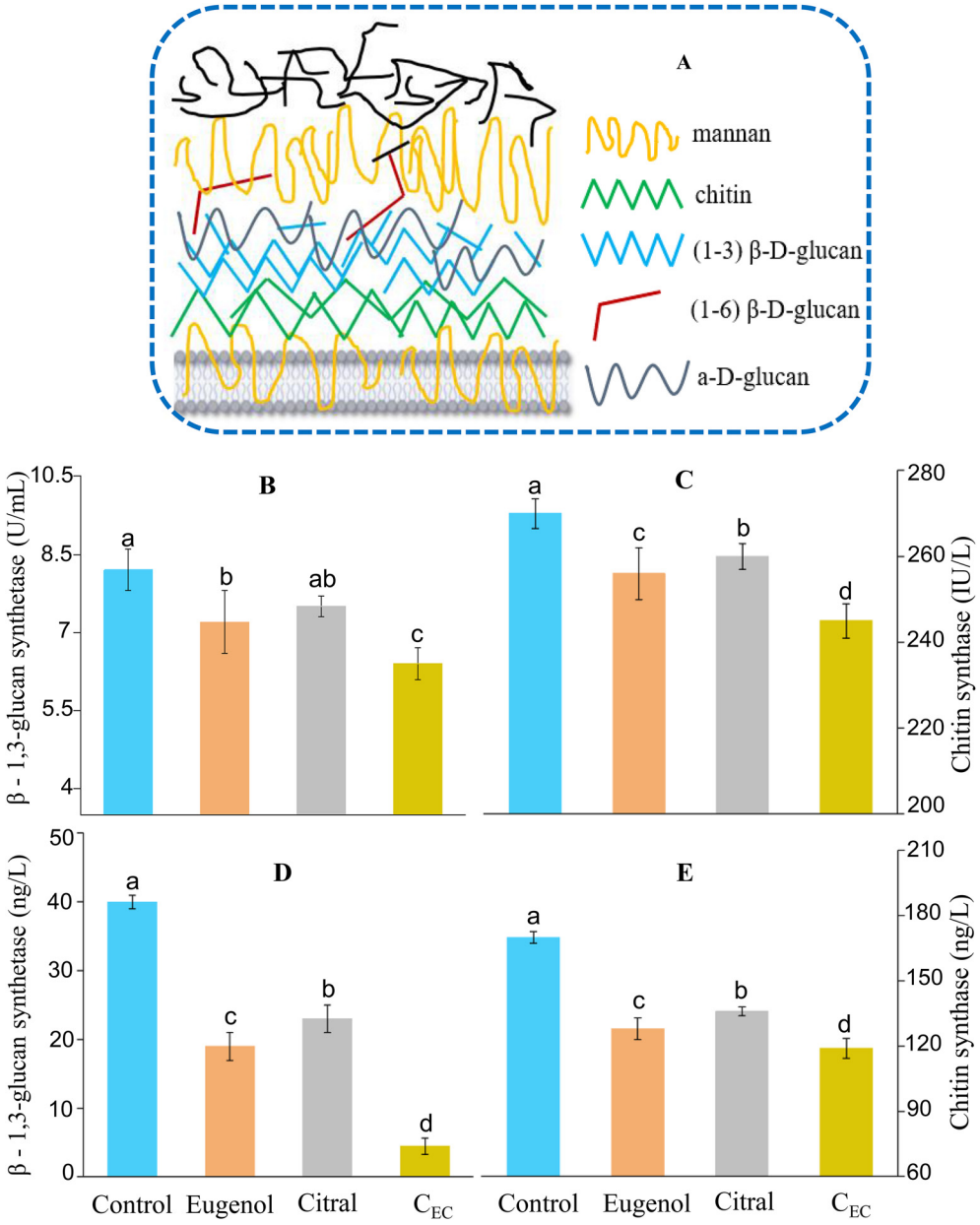

Fig. 1. Changes in activity and content of *β*- (1,3)-glucan synthase and chitin synthase. Error bars represent standard deviations. a-d significant difference ($P < 0.05$) according to Duncan's multiple range test.

2.2. Strain activation

The freeze-dried powder of *P. roqueforti* was first dissolved in a small amount of normal saline, and streaked on the test tube slope of PDA, and cultured at a constant temperature incubator for 48 h at 28 ˚C ± 2 ˚C. The strain obtained after 48 h of culture was the first generation. Some of the strains were stored in the refrigerator at 4 ˚C, while others were transferred to a fresh PDA plate. The fungi were subcultured successively until the 3rd-4 rd generations were obtained for follow-up experiments under the same growth conditions.

2.3. Determination of enzyme activity and content

The spore suspension of *P. roqueforti* (1×10^6 cfu/mL) was added to PDB for incubation. The bacteriostatic agents (eugenol, citral, and C_{EC}) were added to the culture medium after 48 h incubation at 28 ˚C ± 2 ˚C, so that the final concentration of bacteriostatic agents was minimum inhibitory concentration (MIC) (eugenol: 0.06 mg/mL, citral: 0.17 mg/mL and C_{EC}: 0.23 mg/mL). The culture was further incubated for 8 h at 28 ˚C±2 ˚C, and the precipitate was washed with PBS. The lower layer of the sediment was retained for the experiments. The activity and content of β-(1,3)-glucan synthase (GS) and chitin synthase (CS) were determined according to the method described by Hu et al. [10].

2.4. Molecular docking and theoretical calculation

The software Autodock Vina 1.5.6 was used as a molecular docking tool to investigate the binding between C_{EC} and enzymes, and the Iterated Local Search global optimizer was selected [22]. The 2D structure of small molecules was converted into 3D in MOE. Later, the protonation state and hydrogen orientation of the target were optimized by LigX at the conditions of pH 7.0 and 300 K. The binding sites were identified by overlapping proteins with the original template structure. The ligands in the template structure were defined as protein binding sites. The docking workflow adheres to the “induced fitting” protocol, which allows the side chain of the receptor pocket to move while limiting its position according to the conformation of the ligand. The weight used to bind the side chain atom to its original position was 10. Initially, all docked molecular postures were ranked by dG scores. Later, the first thirty postures were refined using a force field, GBVI/WSAdG was scored, and the highest ranked posture was selected as the final mode.

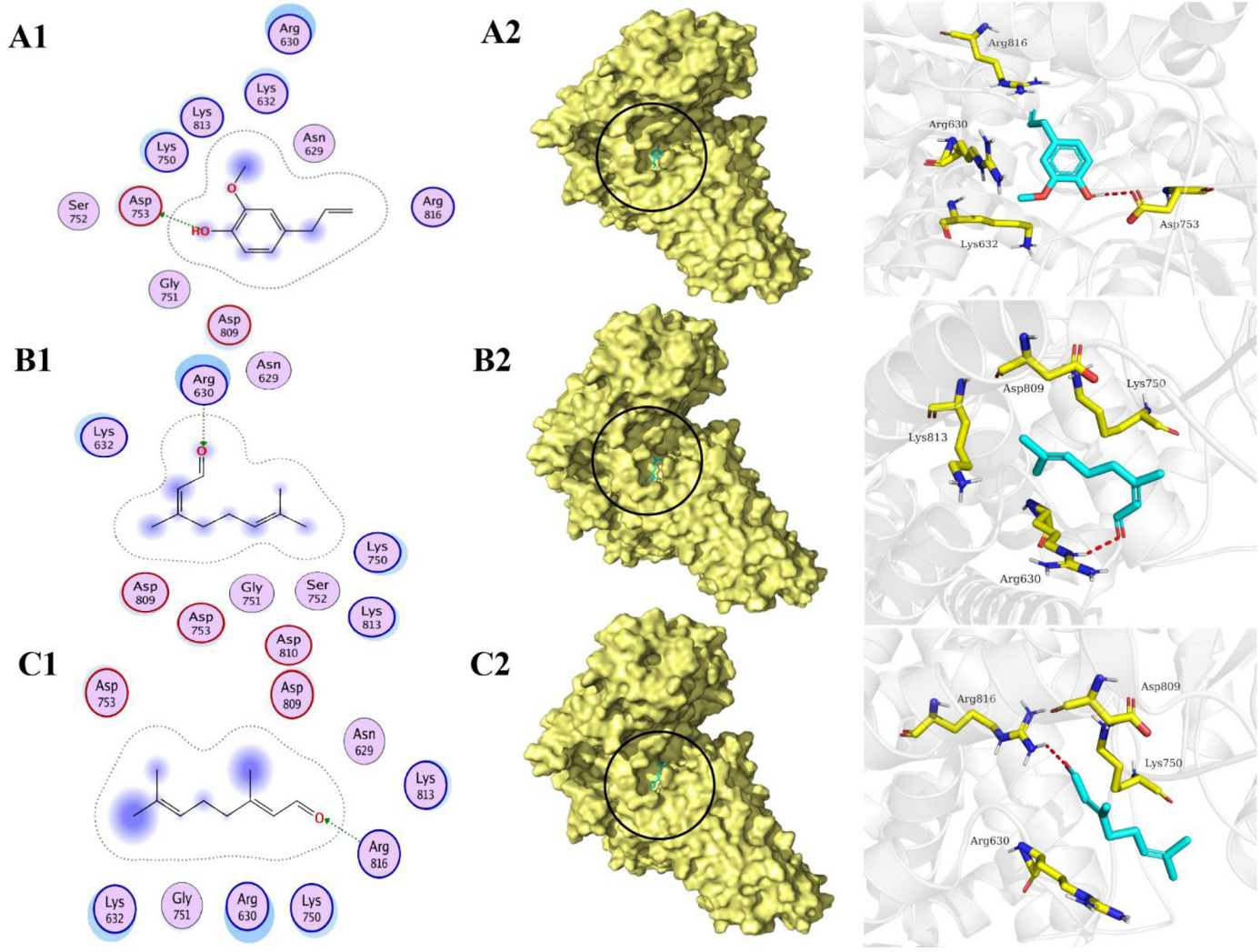

Fig. 2. Molecular docking of eugenol and citral with chitin synthase protein. A1: 2D binding pattern of eugenol and chitin synthase protein. A2: binding model and 3D binding mode of eugenol on the surface of chitin synthase protein molecule. B1: 2D binding pattern of *cis*-citral and chitin synthase proteins. B2: binding model and 3D binding mode of *cis*-citral l on the surface of chitin synthase protein molecule. C1: 2D binding pattern of *trans*-citral and chitin synthase protein. C2: binding model and 3D binding mode of *trans*-citral on the surface of chitin synthase protein.

The Gaussian16 program was used for all the molecular optimization and quantum chemistry calculations, and GaussView was used for structural visualization in this study. The SMD implicit solvent model was used to consider the effect of solvent. DFT-D3 dispersion correction was used to calculate the weak interaction more accurately. The electrostatic potential of the molecular surface was calculated by GaussView calling with CubeGen.

2.5. Determination of ergosterol content

The determination of fatty acid composition was described by Balbino et al. [1] with slight modifications. Briefly, 0.5 mL of methanol/chloroform (2:1, v/v) solution and two steel beads were added to the experimental samples (15–20 mg), which were then submitted to cellular lysis using TissueLyser II (Qiagen, Hilden, Germany). The samples were centrifuged for 10 min at 4000 g, and the supernatant was transferred to a new test tube. Later, 2 mL of 100% chloroform was added to the supernatant and mixed well. 2 mL of 1% (w/v) sodium chloride solution was added, and the solution was harvested for 20 min at 12,000 g. Finally, 10 μL of the lower phase was collected and injected into an RP-C18 column in high-performance liquid chromatography column.

The absorbance of the extracted sterol produced a four-peak spectral absorption pattern (for biomass standardization). The ergosterol content was calculated according to the following formula:

$$Ergosterol\ (\%) = \frac{100}{1 + \left[\left(\frac{A_{230}}{A_{281.5}}\right) \times 0.56\right]}$$

$$24(28)DHE\ (\%) = 100\% - Ergosterol\%$$

where $A_{281.5}$ and A_{230} are the absorbances at 281.5 and 230 nm, respectively.

2.6. Determination of β-galactosidase (βG), alkaline phosphatase (AKP) and ATPase activity (AA)

The experiment was performed as described by Cui et al. [3] with slight modifications. The breakage effect of C_{EC} on the cell membrane permeability of *P. roqueforti* was determined by the change in βG activity. The microbial culture was activated as described in 2.2. A UV-visible spectrophotometer (UV-3820, Shanghai Unocal Instrument Co., Ltd) was used to measure the absorbance at 405 nm and record it as optical density (ODt). The OD value of the control sample (without C_{EC}) was marked as OD_0. The activity of AA was determined by an AA detection

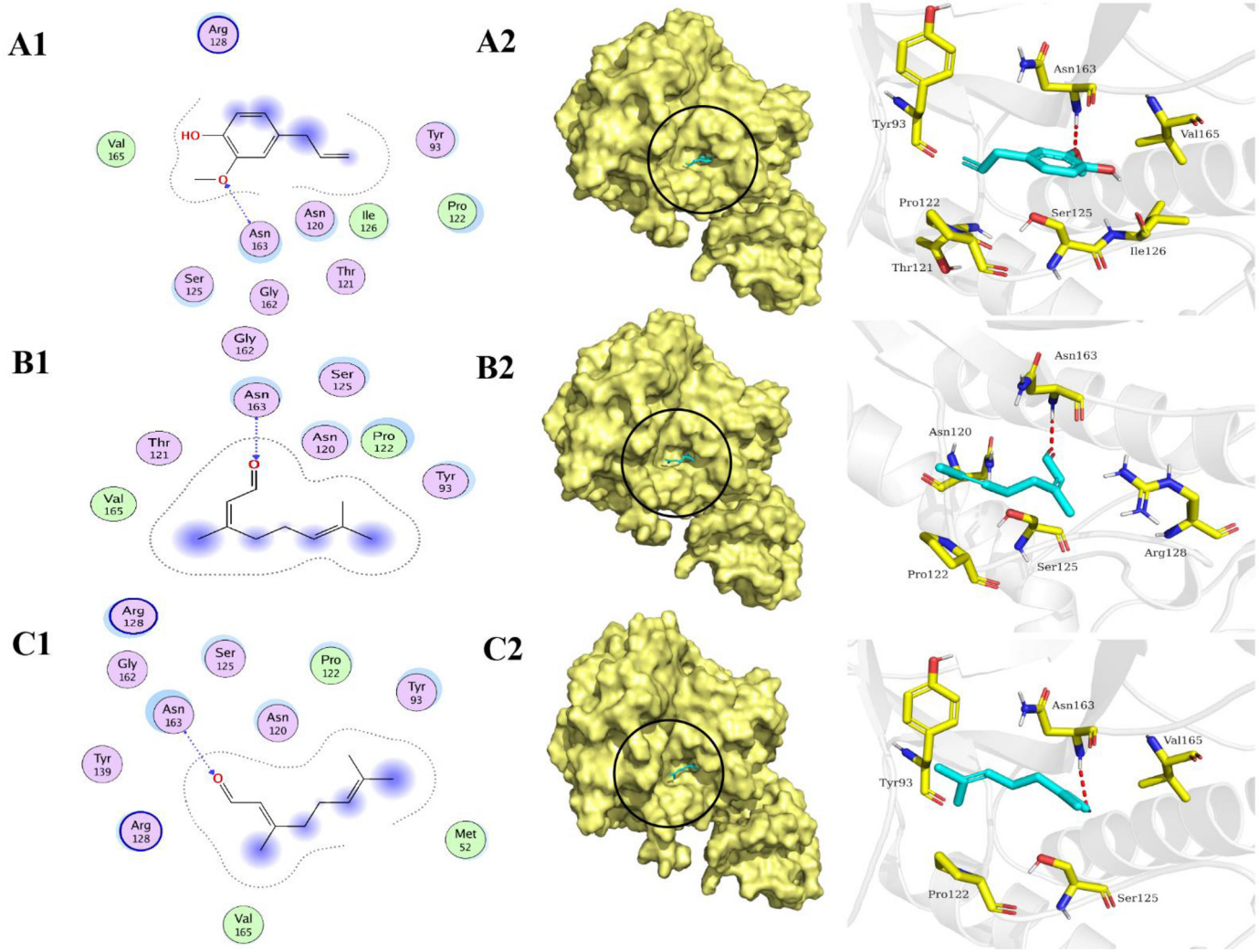

Fig. 3. Molecular docking of eugenol and citral with β-(1,3)-glucan synthase protein. A1: 2D binding pattern of eugenol and β-(1,3)-glucan synthase protein. A2: binding model and 3D binding mode of eugenol on the surface of β-(1,3)-glucan synthase protein molecule. B1: 2D binding pattern of *cis*-citral and β-(1,3)-glucan synthase protein. B2: binding model and 3D binding mode of *cis*-citral l on the surface of β-(1,3)-glucan synthase protein molecule. C1: 2D binding pattern of *trans*-citral and β-(1,3)-glucan synthase protein. C2: binding model and 3D binding mode of *trans*-citral on the surface of β-(1,3)-glucan synthase protein.

kit (Jiangsu Jiancheng Institute of Biological Engineering), and the absorbance at 660 nm was recorded by UV-visible spectrophotometer. An alkaline phosphatase (AKP) detection kit (Jiangsu Jiancheng Institute of Biological Engineering) was used to determine the activity of AKP, and the absorbance at 660 nm was recorded by UV-visible spectrophotometer.

2.7. Determination of the activities of key enzymes in the glycolysis pathway

The experiment was as reported carried out according to Cui et al. [3] with slight modifications. The activities of hexokinase (HK), phosphofructokinase (PFK), and pyruvate kinase (PK) were determined by kit (Jiangsu Jiancheng Bioengineering Institute).

2.8. Determination of intracellular ion leakage and relative conductivity

The 4-day-old mycelium was suspended in 20 mL of 0.85% saline and incubated with eugenol, citral, and C_{EC} at room temperature for 12 h. Later, the mycelium was collected and the leakage of calcium (Ca^{2+}), potassium (K^{+}) and magnesium (Mg^{2+}) ions in the filtrate was determined by atomic absorption spectrometry (iCE 3500, Thermo Scientific) according to the method described by Zhu et al. [35]. Furthermore, the relative conductivity of the solution was measured using a conductivity meter (DDSJ-308S, Guangdong).

2.9. Statistical analyses

All the experimental data were performed in triplicate, and then the average was calculated. Data were analyzed with OriginLab 9.0s. Means were compared by Duncan's new multiple-range test. Statistically significant differences were set at $P < 0.05$.

3. Results and discussion

3.1. Changes in activity and content of β-(1,3)-glucan synthase (GS) and chitin synthase (CS)

GS and CS are key synthases for the synthesis of fungal cell walls. The normal structure and function of the fungal cell wall are destroyed when the activity of these two synthases is inhibited or the content is decreased. Hence, GS and CS play a crucial role in maintaining the integrity of the fungal cell wall.

Fig. 1A shows the main components of the fungal cell wall. The activities of the two enzymes decreased in varying degrees after eugenol, citral, and C_{EC} treatment, especially in the C_{EC} combined treatment group, which decreased by 20.2% and 11.1%, respectively, compared with the control group (Fig. 1B and C). Similarly, the contents of these two enzymes decreased after the treatment with different EO components, especially in the C_{EC} combined treatment group, which decreased by 85.0% and 27.9%, respectively, compared with the control group (Fig. 1D and E). The decrease of the activity and content of GS and CS

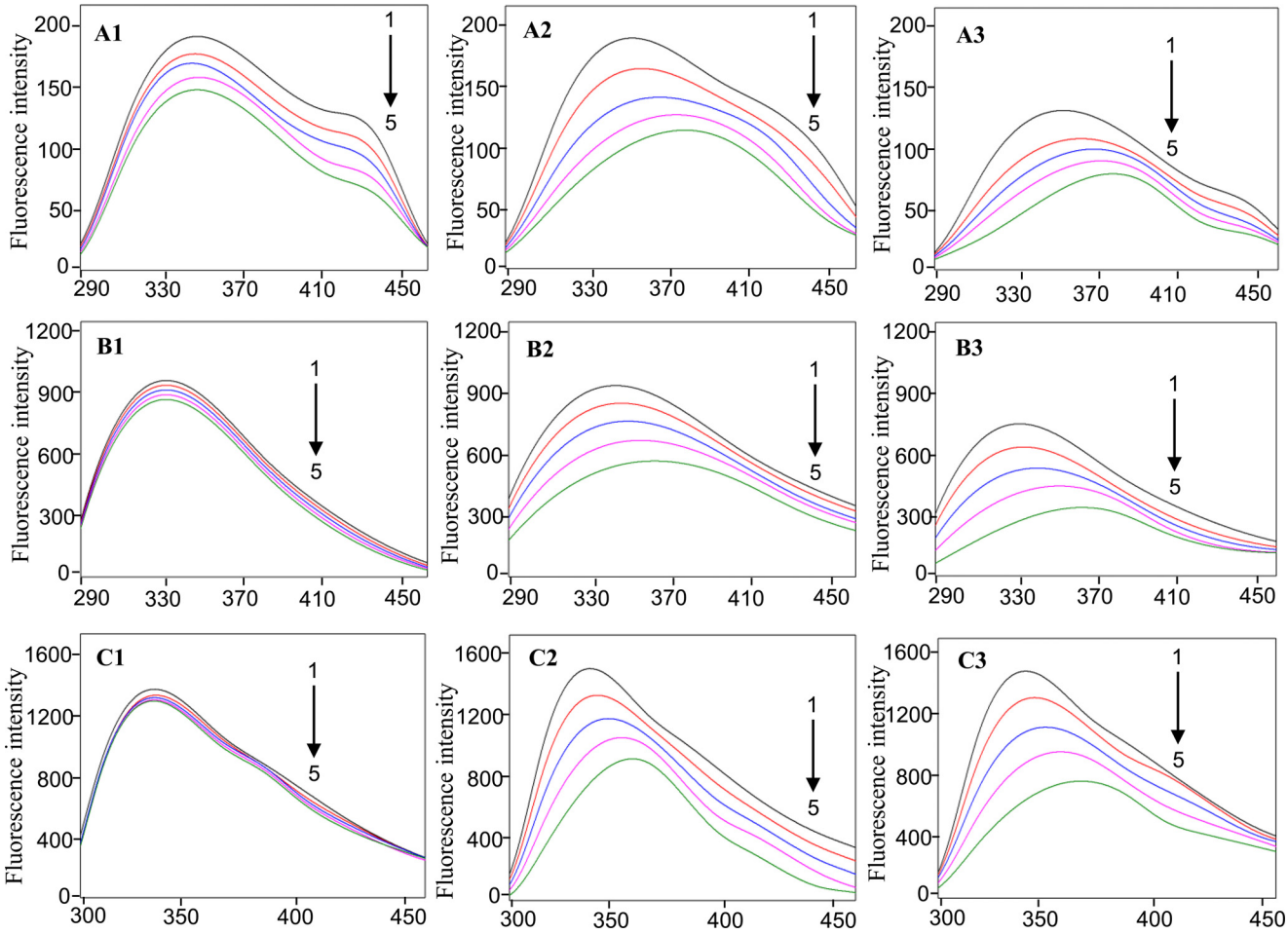

Fig. 4. Fluorescence spectra of amino acid residues Phe (λex = 258 nm), Trp (λex = 280 nm) and Tyr (λex = 296 nm) of *P. roqueforti* membrane protein treated with different concentrations of KI (A1, B1 and C1), eugenol (A2, B2 and C2) and citral (A3, B3 and C3). Curves 1 to 5 correspond to KI concentrations of 0, 5, 10, 15 and 20 mM; Curves 1 to 5 correspond to eugenol and citral concentrations of 0, 1/200, 2/200, 3/200 and 4/200 MIC, respectively.

indicated that the normal function of the synthetic cell wall of *P. roqueforti* was inhibited or the structure of the cell wall was destroyed after the treatment of EO components. Therefore, it can be seen that eugenol and citral can simultaneously act on GS and CS and inhibit their activity and synthesis. Similarly, cinnamaldehyde inhibited the cell wall synthesis of Candida albicans, which was primarily due to the inhibitory effect of cinnamaldehyde on GS [21]. In addition, Ge et al. [8] found that the 3-amino-4-hydroxycoumarin derivative was an effective CS inhibitor, which can significantly inhibit the growth of *A. niger*.

3.2. Molecular docking of eugenol and citral with CS

Chitin is one of the important components of fungal cell walls, but it does not exist in animal or plant cell walls, making CS an ideal target for fungal inhibitors. The binding energies of eugenol, *cis*-citral, and *trans*-citral to CS were −4.76, −4.78 and −4.89 kcal/mol, respectively. It can be observed that *trans*-citral has the best affinity with CS.

Fig. 2A1 and A2 depict the binding mode of eugenol to CS. The hydroxyl group of eugenol can form a hydrogen bond with Asp753. In addition, it could also form weak interactions with Lys750, Lys813, Lys632, Arg816 and Asn629. Fig. 2B1 and B2 show the binding mode of *cis*-citral to CS. Furthermore, the oxygen atom in a (one) carbonyl group of *cis*-citral can form a hydrogen bond with the side chain nitrogen atom of Arg630 as a hydrogen bond acceptor. Similarly, the van der Waals interaction was also formed between *cis*-citral and the surrounding amino acid residues. These amino acid residues mainly include Lys632, Asn629, Lys750, Ser752 and Gly751. Similarly, the oxygen atom in one carbonyl group of *trans*-citral acts as a hydrogen bond acceptor and forms a hydrogen bond with the nitrogen atom in the side chain of Arg816 (Fig. 2C1 and C2).

3.3. Molecular docking of eugenol and citral with GS

The binding energies of eugenol, *cis*-citral and *trans*-citral to GS were −5.05, −4.84 and −4.95 kcal/mol, respectively. Therefore, it can be observed that eugenol has the best affinity with GS.

Fig. 3 (A1 and A2) shows the binding pattern of GS to eugenol. The binding sites of eugenol and GS are spatially complementary. Furthermore, the oxygen atom of eugenol acts as a hydrogen bond acceptor in the formation of a hydrogen bond with Asn163. At the same time, it can also form weak interactions with Tyr 93, Pro 122, Ser 125 and Val 165. Similarly, the enzyme also formed hydrogen bond interactions with *cis*-citral and *trans*-citral. The oxygen atoms of *cis*-citral and *trans*-citral form hydrogen bonds with the nitrogen atoms in the main chain of Asn163, and form a van der Waals weak interaction with the surrounding amino acid residues (Fig. 3 B1, B2 and C1, C2). Moreover, it was observed that

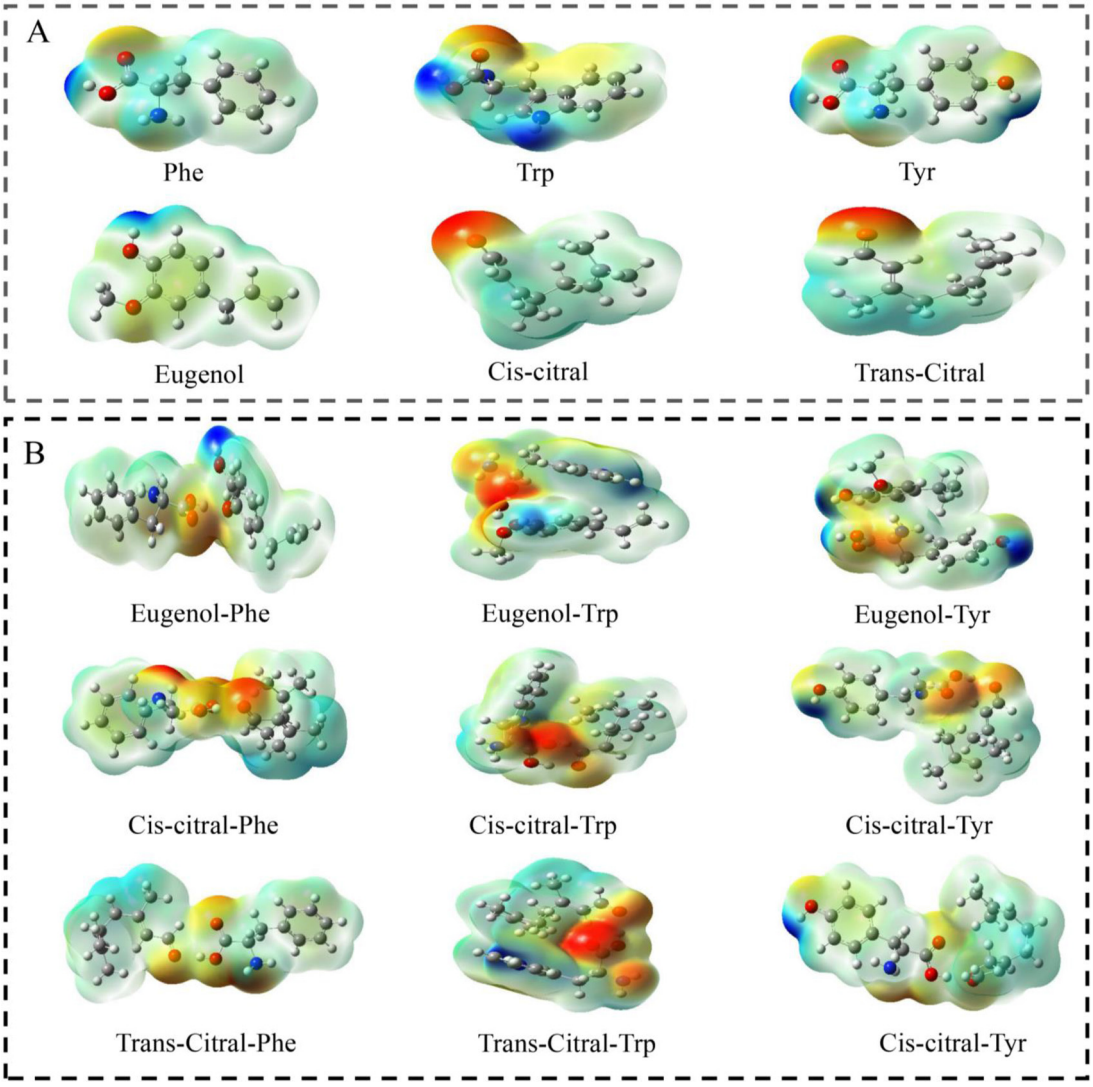

Fig. 5. Potential analysis of the binding of small molecules of eugenol and citral with amino acids. Blue represents positive potential area; red represents negative potential area.

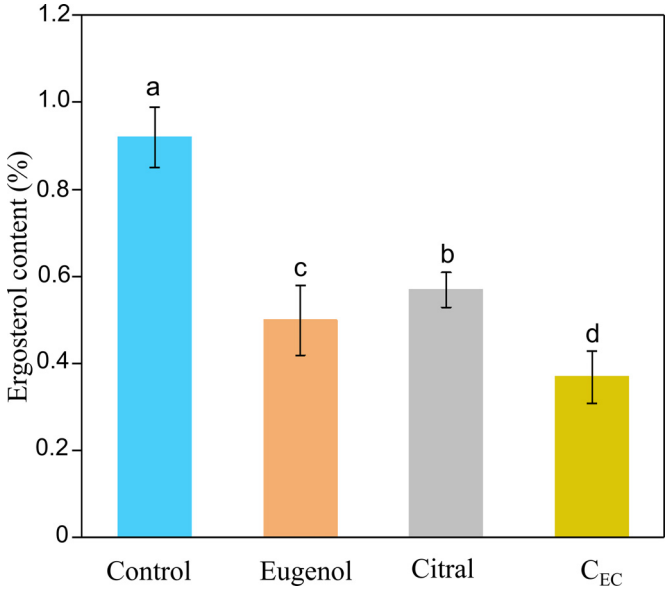

Fig. 6. Changes of ergosterol content. Error bars represent standard deviations. a-d significant difference ($P < 0.05$) according to Duncan's multiple range test.

eugenol and citral small molecules can combine with CS and GS through different active sites.

3.4. Binding of eugenol and citral to amino acids in membrane proteins

The binding of eugenol and citral to membrane proteins was analyzed by fluorescence spectra. Fig. 4 A1, B1, and C1 show the effects of different concentrations of potassium iodide (KI) on the fluorescence emission spectra of tryptophan (Trp), tyrosine (Tyr), and phenylalanine (Phe) residues, respectively. The fluorescence intensity of Phe decreased significantly with the increase of KI content, while Trp and Tyr residues had no obvious quenching effect. This indicates that Phe residues may be located on the outside of the cell membrane, while Trp and Tyr residues may be located in the interior or gap of the cell membrane. The maximum emission wavelength intensity of Phe, Trp and Tyr residues decreased gradually in the presence of different concentrations of eugenol and showed a red shift (Fig. 4 A2, B2, and C2). Similar results (Fig. 4 A3, B3, and C3) were obtained in the citral treatment group. This demonstrates that eugenol and citral small molecules can interact with the amino acids in the cell membrane and change their conformation. Similarly, previous studies have shown that 2R, 3R dihydromyricetin (DMY) interact with amino acids in the cell membrane of *Staphylococcus aureus*, resulting in a significant decrease in membrane fluidity and changes in membrane protein conformation [29].

3.5. Potential analysis of the binding of small molecules of EO with amino acids

The electrostatic potential can be used to predict and elucidate the relative orientation and binding force of the molecules in the complex. The molecules can easily contact with each other by complementary electrostatic potential, which means that the positive region of the electrostatic potential on the molecular surface tends to contact the negative region, and the more positive and negative the positive value is, the stronger the tendency is, which can reduce the overall energy to the maximum extent. Fig. 5 shows the binding sites of eugenol and citral small molecules to Trp, Tyr, and Phe are primarily located around the OH group, which represents the nucleophilic part. The nucleophilic part corresponds to the part of the molecule that tends to give electrons. Therefore, these sites may be the best electrophilic attack sites and potential chemical reaction sites.

3.6. Changes in ergosterol content

Ergosterol is an important component of the fungal cell membrane to maintain normal physiological function and integrity. Therefore, the decrease in ergosterol content may disrupt the homeostasis mechanism of cells and lead to damage to the integrity of cell membrane. Fig. 6 shows that treatments with eugenol, citral, and C_{EC} decreased the ergosterol content in the cell membrane by 45.1%, 35.2% and 58.2%, respectively. It was observed that the decreased rate of ergosterol content in the C_{EC} combined treatment group was significantly ($P < 0.05$) higher than that in the eugenol and citral treatment group at the same concentration.

In previous studies, it was observed that cumin EO could inhibit the synthesis of ergosterol in the cell membrane of *Aspergillus flavus*, resulting in increased permeability of the cell membrane [34].

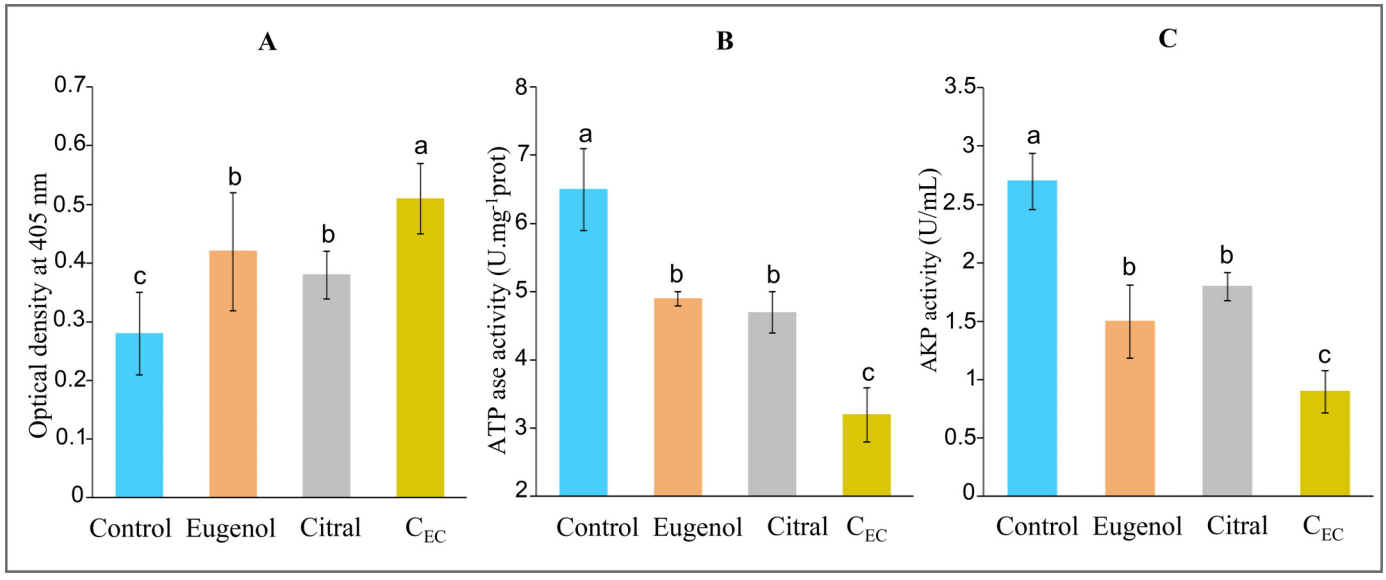

Fig. 7. Changes in the activities of β-galactosidase, ATPase enzyme and alkaline phosphatase (AKP). Error bars represent standard deviations. a-d significant difference ($P < 0.05$) according to Duncan's multiple range test.

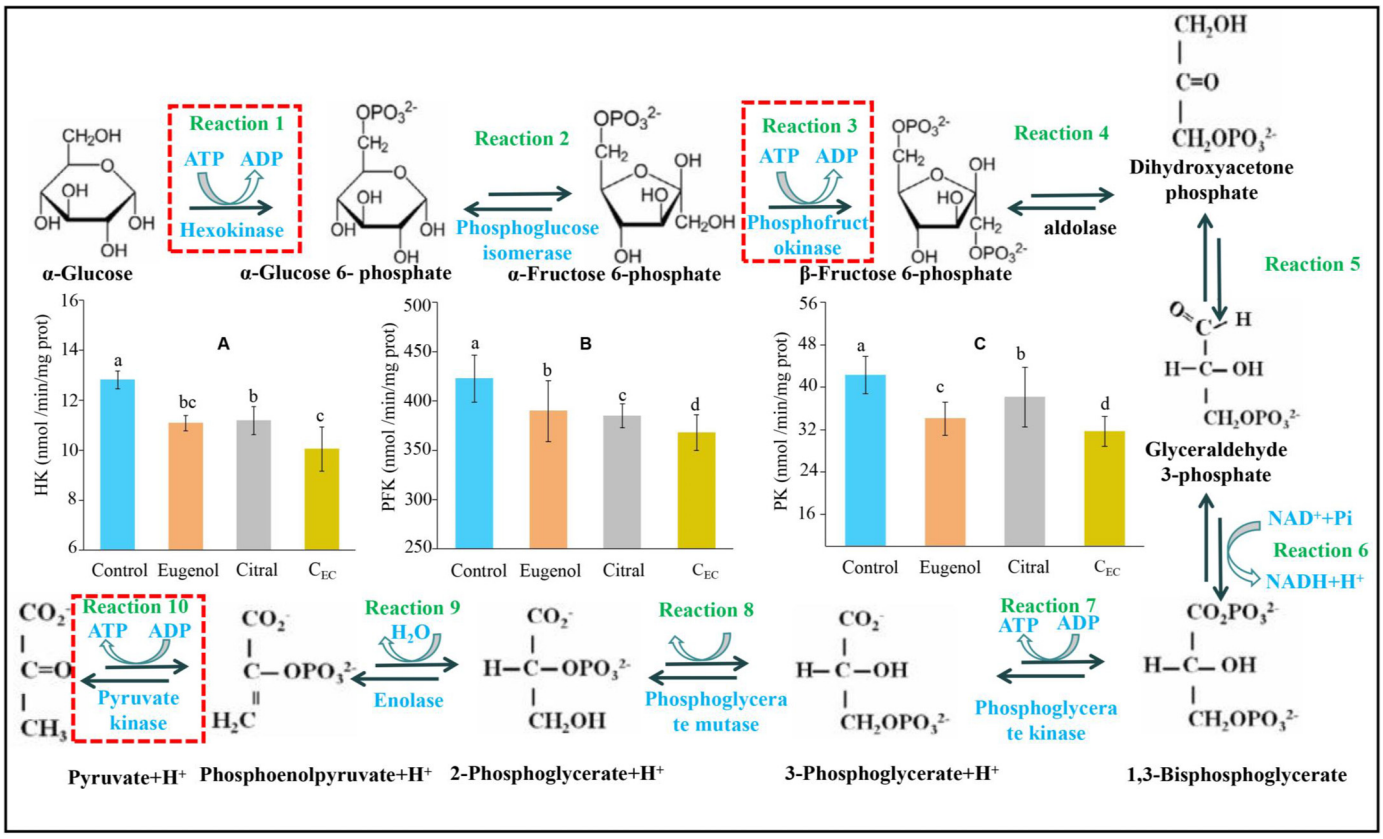

Fig. 8. Effects of C_{EC} on (A) HK, (B) PFK and (C) PK of *P. roqueforti*. (Embden-Meyerhof-Parnas pathway). Error bars represent standard deviations. a-d significant difference ($P < 0.05$) according to Duncan's multiple range test.

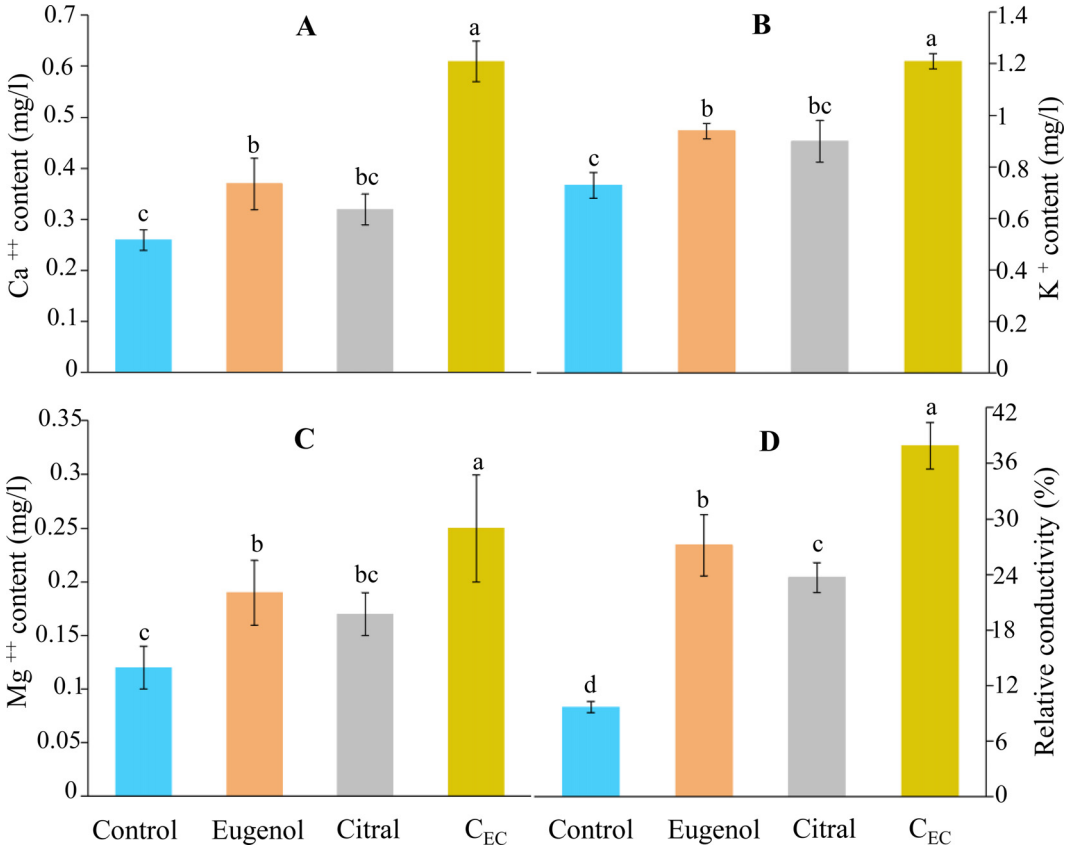

Fig. 9. Leakage of intracellular ions and change of relative conductivity. Note: A, B, C and D are Ca^{2+},K^{+} and $Mg^{2+}$and relative conductivity, respectively. Error bars represent standard deviations. a-d significant difference ($P < 0.05$) according to Duncan's multiple range test.

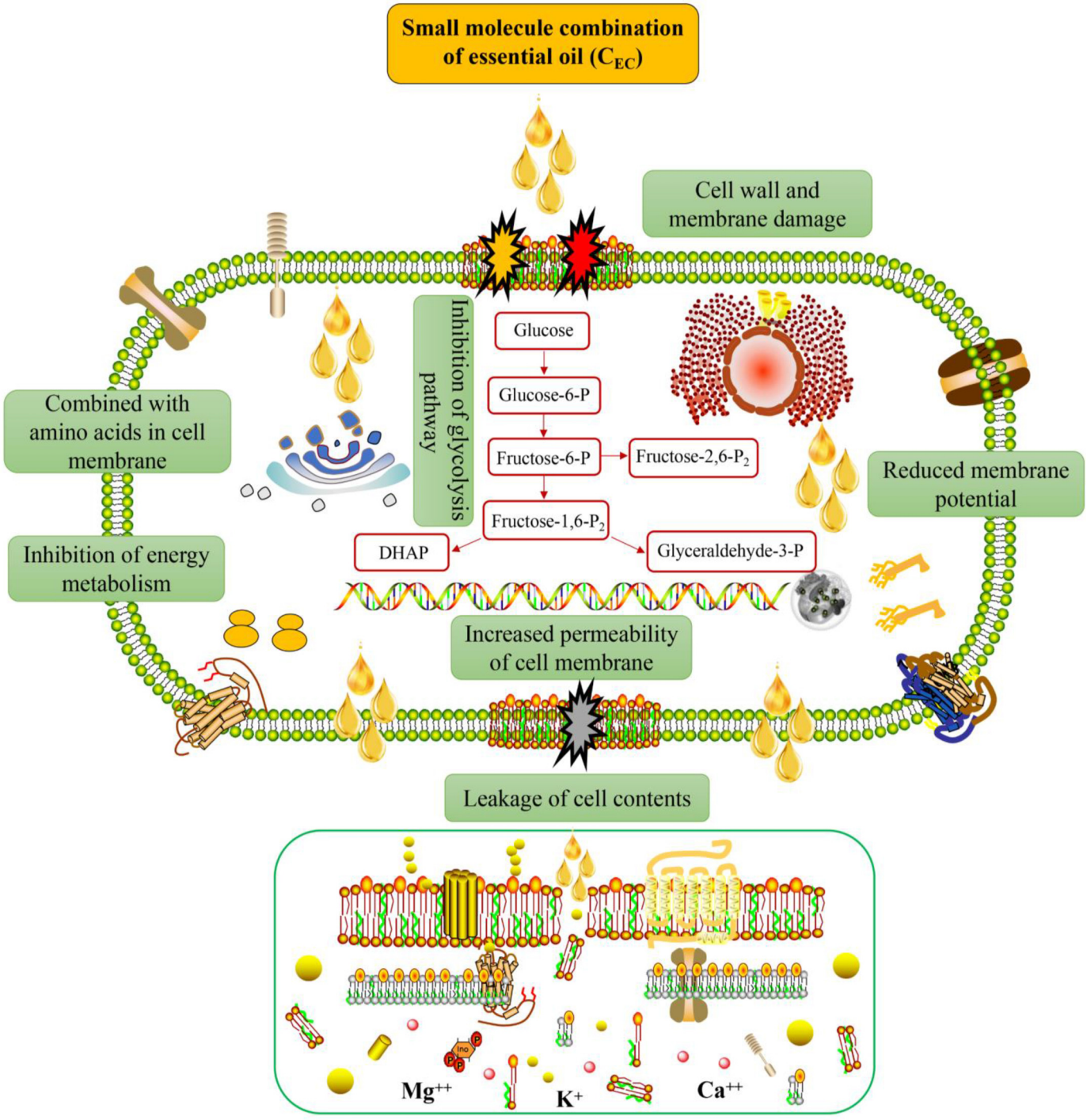

Fig. 10. The antifungal mechanism route of the C_{EC} against *P. roqueforti*.

Similarly, thymol could reduce the ergosterol content in the cell membranes of *Fusarium graminearum* [7]. Furthermore, the authors discovered that CYP51A and KES1 genes played an important role in regulating ergosterol synthesis [30]. Similarly, the lipophilicity of eugenol and citral in the C_{EC} combination contributes to their dissolution in the cell membrane, which reduces ergosterol synthesis and destroys the integrity of the cell membrane. Moreover, when the two are combined, a synergistic is observed, resulting in a significant reduction in the content of ergosterol. Similar to our findings, Huang et al. [11] discovered that cinnamaldehyde and cinnamic acid have a synergistic killing effect on *S. pullorum*, which may be due to the inhibition of glycerophospholipids biosynthesis in the cell membrane.

3.7. Changes in βG, AA, and AKP activity

βG is an important enzyme of microorganisms as it is a key catalyst for energy production and a main source of carbon by decomposing lactose into galactose and glucose. O-nitrophenyl β-D-galactopyranoside (ONPG) is an analog of lactose. It can quickly enter the cell and be hydrolyzed to o-nitrophenol by βG and has characteristic absorption at 405 nm. Fig. 7A shows that the OD value of *P. roqueforti* increased significantly ($P < 0.05$) after C_{EC} treatment indicating that the permeability of the cell membrane increases; thus, allowing ONPG to enter the cell and be hydrolyzed to o-nitrophenol. The increase in cell membrane permeability showed that C_{EC} had a great inhibitory effect on the growth

of the fungal strains studied. This further confirms the previous conclusion that C_{EC} treatment reduces the synthesis of ergosterol, increasing cell membrane permeability.

Fig. 7B and C show that the activities of AA and AKP in the experimental group were significantly lower than that in the control group, especially in the C_{EC} treatment group. After C_{EC} treatment, the AA and AKP enzyme activities of *P. roqueforti* decreased by 50.8% and 63.7%, respectively, compared with the control group. These results demonstrated that C_{EC} can inhibit the activity of endonucleases, and the activities of these two enzymes, which are crucial for the normal growth and energy metabolism of microorganisms. Related studies have confirmed that the decrease of ATP enzyme level is one of the main factors leading to microbial cell death. *Alpinia galanga Rhodes* EO can reduce the AA of *E. coli* O157:H7, inhibit its respiratory metabolism and lead to cell apoptosis [32]. Similarly, Chen et al. [4] also confirmed this conclusion through *Lindera glauca fruit* EO against *Shigella flexneri*.

3.8. Changes in the activities of hexokinase (HK), phosphofructokinase (PFK) and pyruvate kinase (PK) in the EMP pathway

HK, PFK, and PK are the key regulatory enzymes that catalyze the reaction of the Embden–Meyerhof–Parnas (EMP) pathway. These reactions are irreversible and hence, the effect of C_{EC} on the EMP pathway can be investigated by measuring the activities of these three enzymes. Fig. 8 shows the activities of these three enzymes in the C_{EC} treatment group were significantly ($P < 0.05$) lower than that in the eugenol and citral treatment groups. The activities of these three enzymes decreased by 21.9%, 11.8% and 25.6%, respectively, after C_{EC} treatment compared with the control group. This demonstrated that C_{EC} can effectively inhibit the respiratory metabolism of *P. roqueforti* via the EMP pathway.

3.9. Leakage of intracellular ions and changes of relative conductivity

The hydrophobicity of EO will damage the biosynthesis of ergosterol and increase intracellular ion leakage, which may lead to significant changes in cell membrane fluidity and cell contents. This had an adverse effect on the function of organelles, and eventually lead to cell death. Therefore, we measured the leakage of cell contents (Fig. 9). The leakage of important intracellular ions Ca^{2+},K^{+} and Mg^{2+} in the treatment group was significantly ($P < 0.05$) increased compared with the control group (Fig. 9A, B, and C). Especially, the ion leakage of fungal cells in the C_{EC} treatment group increased by 56.3%, 38.0%, and 52.0%, respectively. This phenomenon is further confirmed by the change of conductivity (Fig. 9D). The cell membrane was seriously damaged after C_{EC} treatment, which led to the leakage of cell contents and eventually led to cell death.

Previous studies have also confirmed that *Eugenia stipitata* McVaugh essential oil can destroy the permeability of *Staphylococcus aureus* cell membrane, resulting in cell content leakage and cell death [28]. In addition, a similar of thyme EO was found effective against *Staphylococcus aureus* and *Escherichia coli* [9].

4. Conclusion

The C_{EC} can inhibit *P roqueforti* through different aspects. Firstly, the C_{EC} can inhibit the activity and synthesis of GS and CS. The activity of GS and CS enzymes in the C_{EC} treatment decreased by 20.2% and 11.1%, respectively, and their contents decreased by 85.0% and 27.9%, respectively, compared with the control group. Secondly, the C_{EC} small molecules can combine with tryptophan, tyrosine and phenylalanine in the cell membrane, resulting in cell membrane damage. Potential analysis showed that the binding sites of small molecules to amino acids were mainly located around the OH group. In addition, the C_{EC} also affected the energy metabolism system of *P. roqueforti* and inhibited the glycolysis pathway. Finally, the changes in ergosterol, β-galactosidase, metal ion leakage and relative conductivity confirmed that the cell membrane was damaged. The leakage of Ca^{2+}, K^{+}, and Mg^{2+} ions of fungal cells in the C_{EC} treatment group increased by 56.3%, 38.0% and 52.0%, respectively. The above results showed that the C_{EC} is expected to develop into a new antifungal agent with a synergistic antifungal effect. Simultaneously, the research results have important guiding significance for guiding the development of new natural plant antifungal agents with synergistic antifungal effect. The antifungal mechanism route of the C_{EC} to *P. roqueforti* (Fig. 10).

Declaration of Competing Interest

The authors declare that they have no known competing financial interests or personal relationships that could have appeared to influence thework reported in this paper.

Acknowledgments

This work was supported by the National Natural Science Foundation of China (32202192), Special fund for Taishan Scholars Project, and Shandong Provincial Natural Science Foundation (ZR2020MC213).

References

[1] T.R. Balbino, F.A. da Silveira, R.Z. Ventorim, A.G. do Nascimento, L.L. de Oliveira, W.B. da Silveira, Adaptive responses of Kluyveromyces marxianus CCT 7735 to 2-phenylethanol stress: alterations in membrane fatty-acid composition, ergosterol content, exopolysaccharide production and reduction in reactive oxygen species, Fungal Genet. Biol. 151 (2021) 103561.
[2] R. Cai, M. Hu, Y. Zhang, C. Niu, T. Yue, Y. Yuan, Antifungal activity and mechanism of citral, limonene and eugenol against zygosaccharomyces rouxii, LWT –Food Sci. Technol. 106 (2019) 50–56.
[3] H. Cui, B. Mei, Y. Sun, A. Abdel-Shafi, L. Lin, Antibacterial activity and mechanism of chuzhou chrysanthemum essential oil, J. Funct. Foods 48 (2018) 159–166.
[4] F. Chen, X. Miao, Z. Lin, Y. Xiu, B. He, Disruption of metabolic function and redox homeostasis as antibacterial mechanism of lindera glauca fruit essential oil against shigella flexneri, Food Control 130 (2) (2021) 108282.
[5] G.G.D. de Moura, A.V. de Barros, F. Machado, A.D. Martins, C.M. da Silva, L.G.C. Durango, J. Doria, Endophytic bacteria from strawberry plants control gray mold in fruits via production of antifungal compounds against Botrytis cinerea L, Microbiol. Res. 251 (2021) 126793.
[6] B. dos Reis Gasparetto, R.C. Moreira, R.P.F. de Melo, A. de Souza Lopes, L. de Oliveira Rocha, G.M. Pastore, C.J. Steel, Effect of supercritical CO_2 fractionation of Tahiti lemon (Citrus latifolia Tanaka) essential oil on its antifungal activity against predominant molds from pan bread, Food Res. Int. (2022) 111900.
[7] T. Gao, Z. Hao, W. Zhou, L. Hu, C. Jian, Z. Shi, The fungicidal activity of thymol against fusarium graminearum via inducing lipid peroxidation and disrupting ergosterol biosynthesis, Molecules 21 (6) (2016) 770.
[8] Z. Ge, Q. Ji, C. Chen, Q. Liao, H. Wu, X. Liu, F. Liao, Synthesis and biological evaluation of novel 3-substituted amino-4-hydroxylcoumarin derivatives as chitin synthase inhibitors and antifungal agents, J. Enzyme Inhib. Med. Chem. 31 (2) (2016) 219–228.
[9] Q. He, L. Zhang, Z. Yang, T. Ding, M. Guo, Antibacterial mechanisms of thyme essential oil nanoemulsions against escherichia coli o157:h7 and staphylococcus aureus: alterations in membrane compositions and characteristics, Innovative Food Sci. Emerg. Technol. 75 (4) (2021) 102902.
[10] W. Hu, C. Li, J. Dai, H. Cui, L. Lin, Antibacterial activity and mechanism of Litsea cubeba essential oil against methicillin-resistant Staphylococcus aureus (MRSA), Ind. Crops Prod. 130 (2019) 34–41.
[11] Z. Huang, D. Pang, S. Liao, Y. Zou, P. Zhou, E. Li, W. Wang, Synergistic effects of cinnamaldehyde and cinnamic acid in cinnamon essential oil against S. pullorum, Ind. Crops Prod. 162 (2021) 113296.
[12] H. Ji, H. Kim, L.R. Beuchat, J.H. Ryu, Synergistic antimicrobial activities of essential oil vapours against Penicillium corylophilum on a laboratory medium and beef jerky, Int. J. Food Microbiol. 291 (2019) 104–110.
[13] J. Jian, Y. Xie, Y. Guo, Y. Cheng, Q. He, W. Yao, The inhibitory effect of plant essential oils on foodborne pathogenic bacteria in food, Crit. Rev. Food Sci. Nutr. 59 (2018) 3281–3292.
[14] J. Ju, X. Xu, Y. Xie, Y. Guo, Y. Cheng, H. Qian, W. Yao, Inhibitory effects of cinnamon and clove essential oils on mold growth on baked foods, Food Chem. 240 (2018) 850–855.
[15] J. Ju, Y. Xie, H. Yu, Y. Guo, W. Yao, Synergistic properties of citral and eugenol for the inactivation of foodborne molds *in vitro* and on bread, LWT-Food Sci. Technol. 122 (2020) 109063.
[16] J. Ju, Y. Xie, H. Yu, Y. Guo, W. Yao, Synergistic interactions of plant essential oils with antimicrobial agents: a new antimicrobial therapy, Crit. Rev. Food Sci. Nutr. 2 (2020) 1–12.
[17] J. Ju, Y. Xie, H. Yu, Y. Guo, W. Yao, Application of starch microcapsules containing essential oil in food preservation, Crit. Rev. Food Sci. Nutr. 60 (2020) 2825–2836.

[18] J. Ju, Y. Xie, H. Yu, Y. Guo, Y. Cheng, R. Zhang, W. Yao, Major components in Lilac and Litsea cubeba essential oils kill Penicillium roqueforti through mitochondrial apoptosis pathway, Ind. Crops Prod. 149 (2020) 112349.
[19] S. Kang, X. Li, Z. Xing, X. Liu, X. Bai, Y. Yang, Antibacterial effect of citral on yersinia enterocolitica and its mechanism, Food Control 135 (2021) 108775.
[20] F. Kévin, H. Nolwenn, Z. Marlène, S.P. Lacroix, P. Olivier, R. Karim, G. Vincent, C. Emmanuel, M. Jérôme, Influence of intraspecific variability and abiotic factors on mycotoxin production in penicillium roqueforti, Int. J. Food Microbiol. 215 (2015) 187–193.
[21] M.S.A. Khan, I. Ahmad, S.S. Cameotra, Phenyl aldehyde and propanoids exert multiple sites of action towards cell membrane and cell wall targeting ergosterol in Candida albicans, AMB Express 3 (1) (2013) 1–16.
[22] X. Li, Y. Bai, H. Ji, Z. Jin, The binding mechanism between cyclodextrins and pullulanase: a molecular docking, isothermal titration calorimetry, circular dichroism and fluorescence study, Food Chem. 321 (2020) 126750.
[23] N. Long, K. Rigalma, J.L. Jany, J. Mounier, V. Vasseur, Intraspecific variability in cardinal growth temperatures and water activities within a large diversity of penicillium roqueforti strains, Food Res. Int. 148 (1) (2021) 110610.
[24] S. Rafiee, A. Ramezanian, R. Mostowfizadeh-Ghalamfarsa, M. Niakousari, M.J. Saharkhiz, E. Yahia, Nano-emulsion of denak (oliveria decumbens vent.) essential oil: ultrasonic synthesis and antifungal activity against penicillium digitatum, J. Food Meas. Charact. 16 (1) (2022) 324–331.
[25] C. Sebaaly, A. Jraij, H. Fessi, C. Charcosset, H. Greige-Gerges, Preparation and characterization of clove essential oil-loaded liposomes, Food Chem. 178 (2015) 52–62.
[26] R.B. Suieny, H.B. Antonio, S. Zildenede, N.S. Silveira, C. Macedoab, S.B. Rodriguesdos, F. Debora, J. Munizd, S. Francely, H. dos Santosac, M. Douglas, F. Coutinhocd, C. AssisBezerra, Antibacterial activity of eugenol on the IS-58 strain of Staphylococcus aureus resistant to tetracycline and toxicity in Drosophila melanogaster, Microbial Pathog. 164 (2022) 105456.
[27] J. Thielmann, M. Theobald, A. Wutz, T. Krolo, A. Buergy, J. Niederhofer, P. Muranyi, Litsea cubeba fruit essential oil and its major constituent citral as volatile agents in an antimicrobial packaging material, Food Microbiol. 96 (2021) 103725.
[28] K.C. Wêndeo, M.O. Alisson, S.S. Bianca, B. Valquíria, S.E. Guimarães, C. Karine, V.D.O. SilvaJoão, A.P. Alves, S. Sant'Annada, V.S. Márcia, Antibacterial mechanism of Eugenia stipitata McVaugh essential oil and synergistic effect against Staphylococcus aureus, S. Afr. J. Bot. 147 (2022) 724–730.
[29] Y. Wu, J. Bai, Z. Kai, Y. Huang, G. Hong, A dual antibacterial mechanism involved in membrane disruption and dna binding of 2r,3r-dihydromyricetin from pine needles of cedrus deodara against staphylococcus aureus, Food Chem. 218 (2017) 463–470.
[30] D. Xue, Y. Hang, C. Liu, The fungicidal activity of tebuconazole enantiomers against fusarium graminearum and its selective effect on don production under different conditions, J. Agric. Food Chem. 66 (14) (2018) 3637–3643.
[31] R.J. Yang, S.Y. Miao, N. Cai, J. Chen, Antifungal effect of cinnamaldehyde, eugenol and carvacrol nanoemulsion against penicillium digitatum and application in postharvest preservation of citrus fruit, LWT-Food Sci. Technol. 141 (1) (2021) 110924.
[32] C. Zhou, C. Li, S. Siva, H. Cui, L. Lin, Chemical composition, antibacterial activity and study of the interaction mechanisms of the main compounds present in the alpinia galanga rhizomes essential oil, Ind. Crops Prod. 165 (2021) 113441.
[33] Y. Zhu, C. Li, H. Cui, L. Lin, Encapsulation strategies to enhance the antibacterial properties of essential oils in food system, Food Control 123 (2) (2020) 107856.
[34] Y. Duan, M. Li, H. Zhao, F. Lu, J. Wang, M. Zhou, Molecular and biological characteristics of laboratory metconazole-resistant mutants in Fusarium graminearum, Pestic Biochem Physiol. 152 (2018) 55–61.
[35] W. Zhu, C. Hu, Y. Ren, Y. Lu, Y. Song, Y. Ji, . . . J. He, Green synthesis of zinc oxide nanoparticles using Cinnamomum camphora (L.) Presl leaf extracts and its antifungal activity, J. Environ. Chem. Eng. 9 (6) (2021) 106659.